Effects of Bivalve Shell Particles of Hyriopsis Cumingii on the Performances of Epoxy Resin Studied by Positron Annihilation

Xudong Sun,[1,2,3] Minfeng Zeng,[3] Yun Wang,[3] Genzhong Ji,[1,2,3] Xiandong Yao,[3] Yongmiao Shen,[3] Ning Chen,[3] Fengyuan Yan,[1] Baoyi Wang,[4] Chenze Qi[3]

[1]*Lanzgou Institute of Chemical Physics, Chinese Academy of Science, Lanzhou 730000, People's Republic of China*
[2]*Graduate University of Chinese Academy of Science, Beijing 100049, People's Republic of China*
[3]*Institute of Applied Chemistry, College of Chemistry and Chemical Engineering, Shaoxing University, Shaoxing 312000, People's Republic of China*
[4]*Institute of High Energy Physics, Chinese Academy of Science, Beijing 100049, People's Republic of China*

Received 28 August 2007; accepted 8 February 2008
DOI 10.1002/app.28627
Published online 10 June 2008 in Wiley InterScience (www.interscience.wiley.com).

ABSTRACT: Mussel shell particles sized in micrometer level have been prepared with a ball mill. The X-ray powder diffractrometer (XRD) and Fourier transform infrared (FTIR) results proved that the shell particles contained mainly $CaCO_3$ in the form of aragonite, together with small amount of organic phase. EP modified with shell particles showed a much rougher fracture surface than unfilled EP. The mechanical properties have been improved obviously by adding the shell particles in EP from 1% to 5%. The particle would occupy a number of free volume holes of the EP matrix. This would lead to a decrease in the total free volume concentration of the composites. The particles acted as a bridge to make more molecules interconnected for the good interfacial adhesion, resulting in a reduction of the free volume hole size in the interfacial layers. I_2 reached its highest value when 3% shell particles were added and then decreased as the shell particles content increased. © 2008 Wiley Periodicals, Inc. J Appl Polym Sci 109: 3932–3937, 2008

Key words: free volume; structure–property relations; toughness

INTRODUCTION

Epoxy resins (EP) are used in a variety of applications since their properties, such as thermal stability, mechanical response, low density, and electrical resistance, can be varied considerably. However, epoxy resin often needs to be modified for its brittle nature. Many methods have been used for toughening epoxy resin, such as blending with elastomers[1–3] thermoplastics,[4,5] inorganic rigid particles,[6–8] and others. For the last method, many kinds of particles had been applied successfully, such as $CaCO_3$, SiO_2, TiO_2, ZnO, montmorrillonite, and others.

Basic inorganic materials that are used in nature (such as calcium carbonate, hydroxyapatite, and amorphous silica) are, on their own, very weak. However, when combined with proteins, self-organized into highly ordered structures, and refined over long periods, these basic materials make very strong composites.[9] Such biological materials include bone, teeth, spong spicules, diatoms, and mollusk shells.[10,11] These complex composites contain both inorganic and organic components in their macro-, micro-, and nanostructures.[12] For example, the mollusk shell is a nature ceramic composite with excellent fracture strength and fracture toughness, which are attributed to their unique microstructures. The reported results[13–15] have shown that mollusk shells consist primarily of calcium carbonate ($CaCO_3$), together a relatively small amount of organic matrix material (less than 5%). Calcium carbonate is anionic crystal with relatively low modulus and strength compared with oxide or carbide ceramics. Yet incorporated into the architecture of shells the chalky substance exhibits remarkably high flexural and compressive strength, and unlike man-made ceramics, it is very resistant to fracture.[16] Enlighten by the last toughening method for EP cited above, we recognized that the mollusk shell particles could be a kind of good candidate filler to EP for its own unique properties.

Free volume as defined the difference between the total volume and hypothetically occupied volume, has been considered as an intrinsic parameters that

Correspondence to: C. Qi (qichenze@zscas.edu.cn).
Contract grant sponsor: Zhejiang Provincial Youth Teacher Foundation, Research Project Foundation of the Education Department of Zhejiang Province; contract grant number: 20061156.
Contract grant sponsor: Shaoxing Key Discipline Foundation, China.

will correlate with microstructure and mechanical performance.[17,18] PALS measurements are known to be sensitive at atom-scale free volume holes of polymer materials through formation of the positronium (Ps) atom, which is a bound state of e^+ and e^-. There are two kinds of Ps atoms. The *para*-positronium (*p*-Ps), in which the spins of the positron and electron are antiparallel, has a lifetime of 0.125 ns by self-annihilation in vacuum; while the *ortho*-positronium (*o*-Ps), in which the spins of the positron and electron are parallel, has a longer lifetime of 142 ns in vacuum. The *o*-Ps atoms are preferentially localized in the atom-scale holes and their lifetime is about 1−5 ns because of the pick-off annihilation with electron from the surrounding molecules. The *o*-Ps life time τ_3 correlates to the size of free volume holes and its intensity I_3 provides an indication of the free volume concentration.[19] The relationship between the *o*-Ps lifetime τ_3 and the radius of the free volume hole (R) is summarized in eq. (1)[20,21]:

$$1/\tau_3 = 2\{1 - R/(R + \Delta R) + \sin[2\pi R/(R + \Delta R)]/2\pi\} \quad (1)$$

where R is the radius of the free volume hole, ΔR (= 0.166 nm) is derived from fitting the observed *o*-Ps lifetimes in molecular solids with known hole sizes.

Fractional free volume (f) is defined as product of the *o*-Ps intensity I_3 with the size of free volume hole ($V = 4\pi R^3/3$) according to eq. (2).

$$f = CVI_3 \quad \text{or} \quad f_{app} = VI_3 \quad (2)$$

where C is a coefficient constant. The apparent free volume fraction (f_{app}) is commonly used since the variation rather than the absolute value of free volume fraction is concerned in most studies.

In the present study, we have prepared a series of EP/mussel shell particles composites. The mechanical performance together with the free volume size and concentration for these composites has been carefully examined. The mechanism of reinforcing and toughening by adding mussel shell particles was discussed from the aspect of free volume.

EXPERIMENTAL

Materials

Bisphenol A type epoxy resin (E-51) was purchased from Wuxi Huili Resin Factory (Jiangsu, China). Curing agent 4,4-diamino diphenyl methane (DDM) was purchased from Jiangying Huifeng Chemical Company (Jiangsu, China). The shells used in this study are the bivalve shells of hyriopsis cumingii obtained from Zhuji Pearl Farm in Zhejiang Province, China. The precrushed hyriopsis cumingii shell fragments was grinded by a QLM-80K micro fluidized bed opposed jet mill (Shangyu city Heli Powder Engineering Co., Zhejiang, China) to obtain shell particles sized about 200 meshes. Then the shell particles were thoroughly grinded again by a QM-1SP04 Horizontal Planetary ball mill (Nanjing University Instrument Plant, Nanjing, China) for another 6 h. The result shell particles' size ranges from 0.1 to 4 μm.

Preparation of the composites

Shell particles were suspended in ethyl alcohol with a mass ratio of 1 to 10, and it was sonicated at room temperature for half an hour before it was poured into epoxy resin at 90°C. The resulting mixture was allowed to stir at 90°C for 2 h to remove the solvent, and then sonicated at room temperature for another half an hour. An appropriate amount of DDM (curing agent) was finally added to the mixture at room temperature, which was quickly poured into a preheated steel mold coated with the release agent. After degasification at 90°C for about half an hour, the epoxy/calcium carbonate nanocomposites were allowed to cure at 90°C for 2 h and then at 150°C for 5 h.

Characterization of the composites

The impact tests were performed using a Charpy impact tester (XCJ-5, Chengde Testing Machine Co., China) according to GB/T 2571-1995 (similar to ISO 179-1993) standard procedure. The flexural measurements were performed with a universal materials testing machine (SANS Testing Machine Co., Shenzheng, China) according to GB/T 2570-1995 (similar to ISO 178-1993) standard procedure. Five specimens of each group were prepared and tested.

Morphology of the fracture surface of the composites was examined with a JEM-6360 (Japan) scanning electron microscopy (SEM). All of the scanned samples were coated with gold to improve SEM imaging.

Fourier transform infrared characterization

The Fourier transform infrared (FTIR) spectra of the samples were measured with a FTIR-Nicolet 740 spectrometer in the wave number range of 500–4000 cm^{-1}. Samples for FTIR spectroscopic characterization were prepared by grinding the dry particles with KBr and compressing the mixture to form sheet.

X-ray powder diffractrometer measurement

X-ray powder diffractrometer (XRD) measurements (with a Rigaku D/Max-2550PC) were carried out at

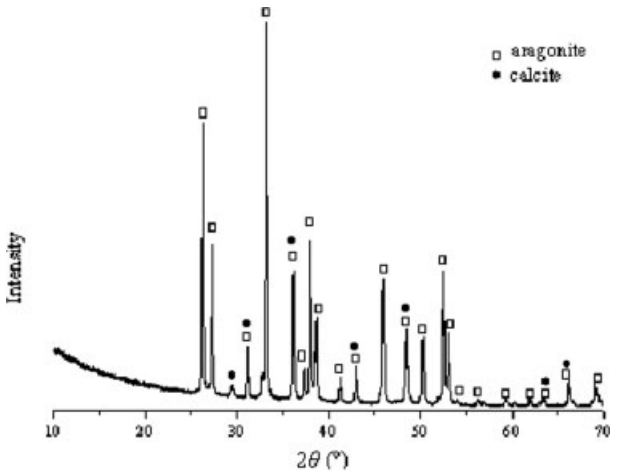

Figure 1 Powder XRD patterns of hyriopsis cumingii shell particles.

room temperature, using Cu Kα radiation generated at 40 kV and 50 mA.

Positron annihilation lifetime spectroscopy

Positron annihilation lifetime spectra (PALS) were recorded in an EG and G ORTEC fast-fast lifetime spectrometer (ORTEC Co., Tennessee, USA) with a FWHM = 190 ps for a ^{60}Co prompt peak of 1.18 MeV and 1.33 MeVγ ray. A 6×10^5 Bq positron source (^{22}Na) was deposited in a piece of Kapton, which was sandwiched between two identical composite samples. All PALS measurements were performed at room temperature, and each spectrum contained about 10^6 counts. All of the PALS spectra were analyzed with a three-component computer-fitting program PATFIT-88.

RESULTS AND DISCUSSION

Structure analysis of the shell particles

Figure 1 gives the XRD pattern of the shell particles. The XRD results showed that the crystal of the shell particles is mainly aragonite, with a small fraction of calcite. Other researchers reported similar results.[22]

Figure 2 shows the comparison of FTIR spectrum of the shell particles used in this work and common $CaCO_3$. For common $CaCO_3$ (sample a), it is seen that, the absorption bands of CO_3^{2-} are observed at the wave number 711 (ν_4-CO_3^{2-}), 874 (ν_2-CO_3^{2-}), 1072 (ν_1-CO_3^{2-}), 1460 (ν_3-CO_3^{2-}), 1792 (ν_3-CO_3^{2-}), and 2520 cm^{-1} ($\nu_1 + \nu_3$), which are the common feature of the CO_3^{2-} ions in $CaCO_3$. The absorption bands in the range 3500–3700 cm^{-1} suggest that these bands are due to the presence of water content. ν_4-CO_3^{2-} absorption at wave number 711 cm^{-1} could be a peak of calcite. As for sample b, the absorption bands of CO_3^{2-} ions in shell particles (sample b) are observed at the wave number 693 (ν_4-CO_3^{2-}), 713 (ν_4-CO_3^{2-}), 860 (ν_2-CO_3^{2-}), 1072 (ν_1-CO_3^{2-}), 1460 (ν_3-CO_3^{2-}), 2520 cm^{-1} ($\nu_1 + \nu_3$). ν_4-CO_3^{2-} absorption at the wavenumber 693 cm^{-1} and 713 cm^{-1} could be the peaks of aragonite. Unlike common $CaCO_3$, the new absorption peaks at 2856 cm^{-1}, 2932 cm^{-1} could be assigned to the C—H aliphatic stretching of the organic phase (protein-rich material) of the shell particles. The medium absorption peak at 1784 cm^{-1} of sample b could be mainly attributed to the C=O stretching of the organic phase of the shells. And the weak absorption peak at 1030 cm^{-1} of sample b could be attributed to the C—H bending of the organic phase of the shells.

The XRD and FTIR results proved that the shell particles contained mainly $CaCO_3$ in the form of aragonite, together with small amount of organic phase. The inorganic aragonite looks like ''brick,'' and the organic phase (protein-rich material) looks like ''mortar.'' The superior properties of shell to common $CaCO_3$ were mainly attributed to such ''brick-and-mortar'' microstructure, which has developed through millions of years of evolution and nature selection.[15,23]

Free volume properties of the composites

The positron lifetime spectra in EP/shell particles composites as a function of shell particles content have been measured. The shell particles weight percentage dependence of the *o*-Ps lifetime τ_3, its intensity I_3, and apparent free volume fraction f_{app} are shown in Figure 3–5. Previous studies[24–26] had shown that in the case of thermosetting-based composites, chains are restricted in the rigid network structure (in which chain units connect with chemical bond) and its mobility depend much more on the

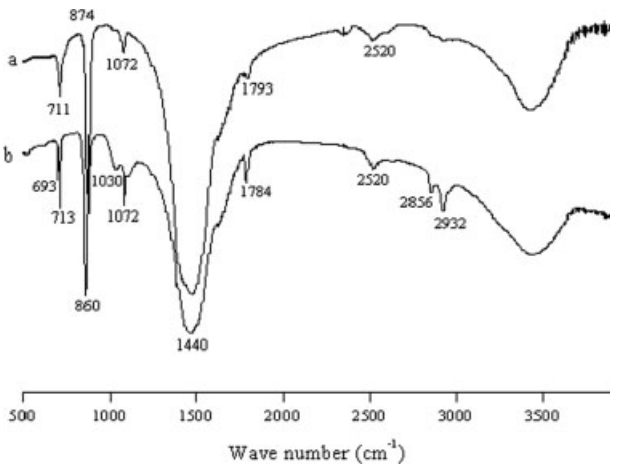

Figure 2 The FTIR spectra of the particles: (a) $CaCO_3$ and (b) hyriopsis cumingii shell particles.

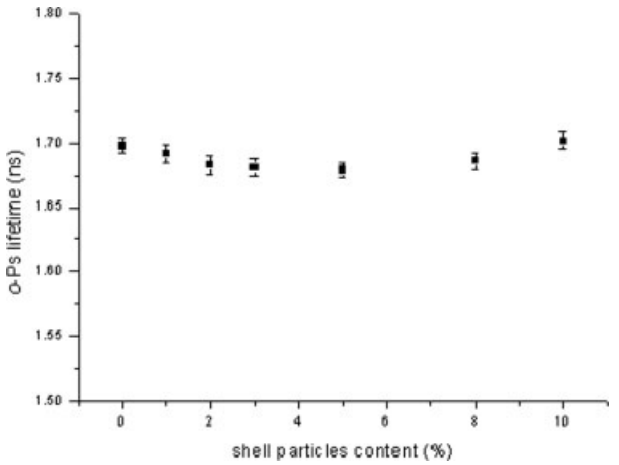

Figure 3 Variation of τ_3 with content of shell particles.

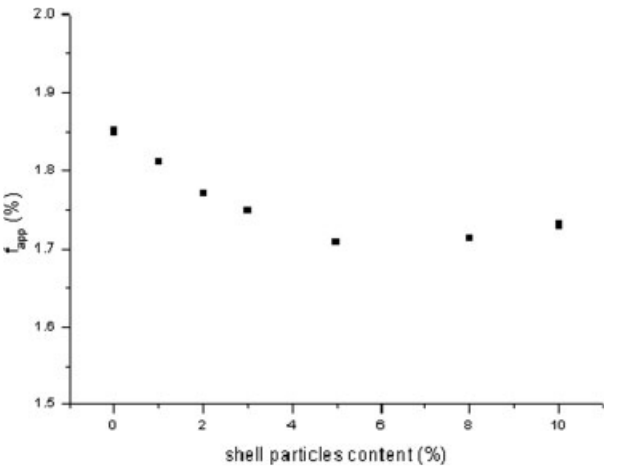

Figure 5 Variation of the apparent free volume f_{app} with content of shell particles.

properties of network, such as the chemical structure and crosslinking density of network. The size and concentration of the free volume holes are mainly determined by the backbone structure, which strongly depend on the conversion of cure reaction. As shown in Figure 3, the *o*-Ps lifetime τ_3 showed a decrease with increasing the shell particles weight percentage from 1% to 5% and then a increase with further addition of shell particles (>5%). The *o*-Ps intensity I_3 decreased with addition of shell particles (as shown in Fig. 4). According to eq. (1), the average radius R of the free volume holes of pure EP matrix could be calculated and its value was 0.2554 nm.[24] In this study, the added shell particle was in micrometer level. It was hard to enter the free volume hole of EP matrix for its big size. And so, the added particle could occupy a number of free volume holes of the EP matrix and inducing the deformation of the network. This would lead to a decrease in the total free volume concentration of the composites. Therefore, it was not difficult to understand why the I_3 decreased as the shell particles were filled. When the weight percentage of shell particles is low, the particles can be fairly well dispersed in EP matrix. The organic phase of the shell particles is much help to improve the interfacial adhesion between the particles and EP matrix. The particles played a role as a bridge among the EP molecules and make more molecules interconnected in the interfacial layers. It would result in a good interfacial adhesion and a reduction of the free volume hole size in the interfacial layers. For this reason, the mean free volume size of the composites would decrease. When more shell particles were added, they would aggregate to form much larger particles, resulting in reduction of the interfacial interaction between the particles and the polymer matrix. Accordingly, the *o*-Ps lifetime τ_3 then increases with further addition of shell particles (>5%). From Figure 5, f_{app} showed a decrease as the filler content was increased. The apparent free volume fraction is a comprehensive reflect of the changes in free volume hole size and its concentration.

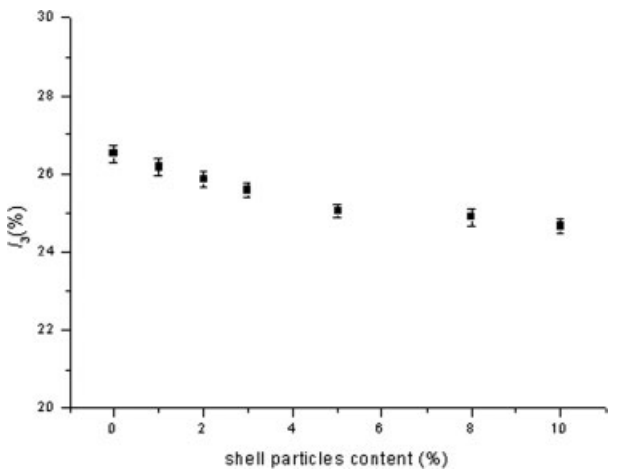

Figure 4 Variation of I_3 with content of shell particles.

The variations of the second lifetime component intensity (I_2) are shown in Figure 6. In the interfacial layers, besides the *o*-Ps annihilation in the free volume holes of EP molecules, the positron is also expected to annihilate in the interfacial layers between particles and EP matrix and attributed to the second lifetime component. The interfacial property can also reflect from the second lifetime component intensity (I_2).[25–27] I_2 reached its highest value when 3% shell particles were added and then decreased as the shell particles content increased. This means more interfacial layers formed between the uniformly dispersed shell particles and EP matrix. It was similar with the results observed in other polymer nanocomposites.[25–27] Nanoparticles have

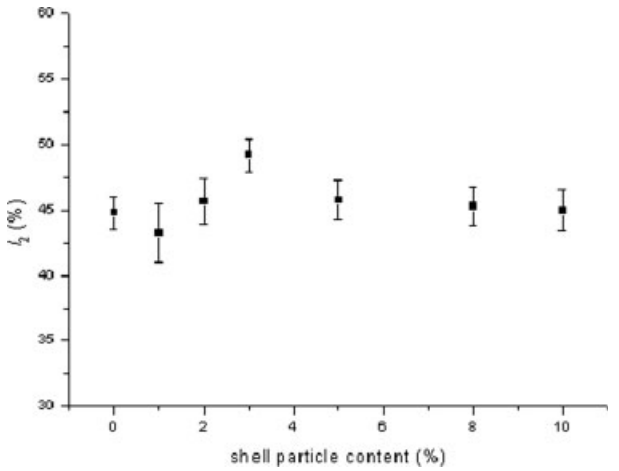

Figure 6 Variation of the intermediate lifetime intensity I_2 with content of shell particles.

very large specific surface area and surface activity. More interfacial layers would form between the uniformly dispersed nanoparticles and polymer matrix. Therefore, more positrons would annihilate in the interfacial layers and then I_2 increased. However, in this study, the shell particles size is mainly in micrometer level. The increase of I_2 was mainly attributed to the good interfacial interaction between the shell particles and EP matrix. As mentioned earlier, mollusk shell particles consist primarily of $CaCO_3$, together with a relatively small amount of organic matrix material. The organic phase of the shell particles is much help to improve interfacial adhesion. More interfacial layers would form between the uniformly dispersed shell particles and EP matrix. Accordingly, similar trends of I_2 were observed in this system with in other nanocomposites.

Toughening and reinforcing behavior

The mechanical properties of EP containing different amounts of shell particles were summarized in Table I. It can be seen from Table I that the mechanical properties have been improved obviously by adding the shell particles in EP from 1 to 5%. When the weight percentage of shell particles in EP is 2%, the toughness and the modulus achieve 11.1 kJ/m^2 and 3.47 $\times$ 10^3 MPa, increasing 37 and 26% comparing with EP, respectively. Figure 7 showed the SEM observation results of the impact facture surface of the composites. Unfilled EP basically showed a smooth and brittle fracture surface [Fig. 7(a)]. EP modified with shell particles showed a much rougher fracture surface [Fig. 7(b,c)] than unfilled EP. This result showed that good interfacial adhesion between EP and shell particles will bring about an increase of toughness.

The properties are related to the microstructure of the composites. According to the results reported by Jean et al., one correlation is that the fracture toughness increases as the free volume fraction increase for EP base composites.[28] The composites can provide more room for the segmental motion with higher free volume fraction, leading much impact energy to be absorbed. However, in this system, both the toughness and modulus of the filled EP were higher than pure EP though a decrease of apparent free volume fraction was observed. To explain this phenomenon, the interfacial property of the composites must be taken into account except the free volume fraction. As mentioned earlier, with addition of appropriate amounts of shell particles, more interfacial layers and stronger interfacial adhesion formed between the uniformly dispersed shell particles and EP matrix. It was much helpful to stress transitions between the matrix and particles while the composites were performed with outside force. On the other hand, the good properties of the shell particles themselves should be considered. Many works[15,23,29,30] showed that shells had much better mechanical properties (both fracture toughness and hardness) than common $CaCO_3$ minerals (calcite and aragonite). Therefore, both the modulus and toughness of the composites will be upgraded by adding appropriate amounts of shell particles to EP. For example, as compared with other reported EP/nano-$CaCO_3$ blend system,[31] EP filled with such shell particles showed near toughness but higher flexural properties.

CONCLUSIONS

The toughening and reinforcing behavior of shell particles in micrometer level to EP matrix has been studied from the aspect of free volume. The added shell particle was hard to enter the free volume hole of EP matrix for its size in micrometer level. The particle could occupy a number of free volume holes of the EP matrix. Accordingly, this would lead to a decrease in the total free volume concentration of the composites. The organic phase within shell par-

TABLE I
Mechanical Property of the Composites

Shell particles weight percentage (%)	Impact strength (kJ/m^2)	Flexural strength (MPa)	Flexural modulus ($\times$10^3 MPa)
0	8.1 ± 0.4	112.4 ± 4.3	2.75 ± 0.09
1	12.1 ± 0.6	131.6 ± 6.1	3.31 ± 0.11
2	11.1 ± 0.6	140.7 ± 4.8	3.47 ± 0.09
3	11.5 ± 0.4	137.8 ± 7.2	3.44 ± 0.1
5	11.4 ± 0.7	123.6 ± 6.8	3.41 ± 0.11
8	10.3 ± 0.5	119.3 ± 8.4	3.34 ± 0.08
10	8.3 ± 0.4	116.8 ± 7.8	3.21 ± 0.09

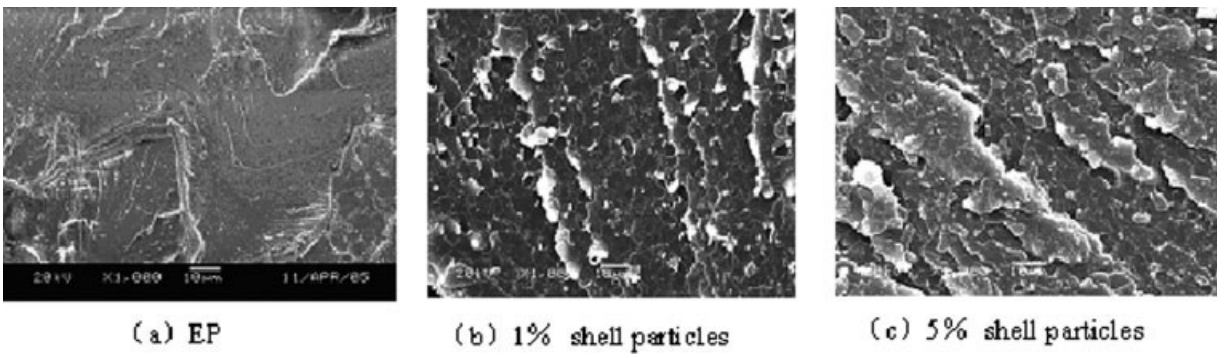

Figure 7 Scanning electron microscopic observation of impact fracture of the EP/shell particle system.

ticles is much help to improve the interfacial adhesion between the shell particles and EP matrix. More interfacial layers would form between the uniformly dispersed shell particles and EP matrix. Similar trends of I_2 were observed in this system with in other nanocomposites. This good interfacial property was much helpful to stress transitions between the matrix and particles while the composites were performed with outside force. On the other hand, shell particles themselves had good properties (both fracture toughness and hardness). Thus, the composites with appropriate amounts of shell particles filled could achieve higher impact strength and modulus than pure EP.

References

1. Bagheri, R.; Williams, M. A.; Pearson, R. A. Polym Eng Sci 1997, 37, 245.
2. Verchere, D.; Sautereau, H.; Pascault, J. P. J Appl Polym Sci 1990, 41, 467.
3. Verchere, D.; Pascault, J. P.; Sautereau, H.; Moschiar, S. M.; Riccardi, C. C.; Williams, R. J. J. J Appl Polym Sci 1991, 42, 701.
4. Bucknall, C. B.; Gilbert, A. H. Polymer 1989, 30, 213.
5. Takao, I.; Masao, T. J Appl Polym Sci 1991, 43, 463.
6. Zheng, Y. P.; Zheng, Y.; Ning, R. C. Mater Lett 2003, 57, 2940.
7. Iijima, T.; Nishina, T. J Appl Polym Sci 1996, 60, 37.
8. Goyanes, S.; Rubiolo, G.; Marzocca, A.; Salgueiro, W.; Somoza, A.; Consolati, G. Polymer 2003, 44, 3193.
9. Kuhn-Spearing, L. F.; Kessker, H.; Chateau, E.; Ballarin, R.; Heuer, A. H. J Mater Sci 1996, 31, 6583.
10. Weiner, S.; Wagner, H. D. Annu Rev Mater Sci 1998, 28, 271.
11. Weiner, S.; Addadi, L. J Mater Chem 1997, 7, 689.
12. Lowenstam, H. A.; Weiner, S. On Biomineralisation; Oxford University Press: New York, 1989.
13. Bond, G. M.; Richman, R. H. J Mater Eng Perform 1995, 4, 334.
14. Kaplan, D. L. Biomaterials 1998, 3, 232.
15. Mayer, G. Mater Sci Eng C 2006, 26, 1261.
16. Currey, J. D. Proc R Sot Lond B 1977, 196, 443.
17. Ito, K.; Kobayashi, Y.; Appl Phys Lett 2003, 82, 654.
18. Hu, Y. H.; Qi, C. Z.; Liu, W. M.; Wang, B. Y.; Zheng, H. T.; Sun, X. D.; Zheng, X. M. J Appl Polym Sci 2003, 90, 1507.
19. Jean, Y. C. Microchem J 1990, 42, 72.
20. Tao, S. J. J Chem Phys 1972, 56, 5499.
21. Eldrup, M.; Lightbody, D.; Sherwood, J. N. Chem Phys 1981, 63, 51.
22. Udomkan, N.; Limsuwan, P. Mater Sci & Eng: C 2008, 28, 316.
23. Tang, H.; Barthelat, F.; Espinosa, H. D. J Mech Phys Solids 2007, 55, 1410.
24. Zeng, M. F.; Sun, X. D.; Yao, X. D.; Ji, G. Z.; Chen, N.; Wang, B. Y.; Qi, C. Z. J Appl Polym Sci 2007, 106, 1347.
25. Yu, D. H.; Wang, B.; Feng, Y.; Fang, Z. P. J Appl Polym Sci 2006, 102, 1509.
26. Wang, B.; Qi, N.; Gong, W.; Li, X. W.; Zheng, Y. P. Radiation Phys Chem 2007, 76, 146.
27. Liu, L. M.; Fang, P. F.; Zhang S. P.; Wang, S. J Mater Chem Phys 2005, 92, 361.
28. Jean, Y. C.; Deng, Q.; Nguyen, T. T. Macromolecules 1995, 28, 8840.
29. Currey, J. D. Proc R Soc London 1977, 196, 443.
30. Jackson, A. P.; Vincent, J. F. V.; Turner, R. M. Proc R Soc London 1988, 234, 415.
31. Li, L.; Zou H. K.; Shao L.; Wang G. Q.; Chen, J. F. J Mater Sci 2005, 40, 1297.